16th World Conference on Earthquake Engineering, 16WCEE 2017
Santiago Chile, January 9th to 13th 2017
Paper N° 4645
Registration Code: S-R1466025774

CORRELATION OF SPECTRAL VALUES IN WORLDWIDE SUBDUCTION ZONE EARTHQUAKES

A. Bebamzadeh[(1)], M. Fairhurst[(2)], C. E. Ventura[(3)]

[(1)] Research Associate, Civil Engineering, UBC Vancouver, armin@civil.ubc.ca
[(2)] Graduate Research Assistant, Civil Engineering, UBC Vancouver, fairhurstmike@gmail.com
[(3)] Professor, Civil Engineering, UBC Vancouver, ventura@civil.ubc.ca

Abstract

Ground motion prediction equations (GMPEs) have been developed to predict the mean and standard deviation of the logarithm of spectral acceleration for a wide variety of earthquake types and locations. An example is the PEER NGA-West1 and West2 GMPEs, which were developed for shallow, crustal events typical of locations such as California. Many researchers have extended these models by determining the correlation between response spectral values at different periods. These results can be used to develop conditional spectra (CS) and conditional mean spectra (CMS), which are becoming more commonly used for ground motion selection and scaling. Currently, correlation coefficients developed considering only shallow, crustal events are commonly used to develop CS and CMS. Whether or not these correlations and corresponding equations are valid for other tectonic regimes, such as subduction zones, is currently unknown.

This paper evaluates the response correlation values from a large database of worldwide subduction zone earthquakes, comprising over 4400 events recorded in worldwide subduction regimes, including the recent Tohoku, Japan (M_w 9.0, 2011), Maule, Chile (M_w 8.8, 2010), and Sumatra, Indonesia (M_w 9.1, 2004) earthquakes. The results are then compared to the correlations observed for shallow, crustal events. The results of this study can be used to develop CS and CMS in worldwide subduction tectonic zones, such as those found in South and Central America, Japan, and the Pacific Northwest of North America.

Keywords: Subduction zone earthquakes, epsilon correlation, conditional spectrum, ground motion prediction equations

1. Introduction

Ground motion prediction equations (GMPEs) have been developed to predict the mean and standard deviation of the logarithm of spectral acceleration for a wide variety of earthquake types and locations. An example is the PEER NGA-West1 and West2 GMPEs, which were developed for shallow, crustal events typical of locations such as California [1]. Many researchers have extended these models by determining the correlation between response spectral values at different periods [2, 3]. These results can be used to develop conditional spectra (CS) and conditional mean spectra (CMS) [4], which are becoming more commonly used for ground motion selection and scaling. Currently, the correlation coefficients developed by Baker and Jayaram [3] are commonly used to develop CS and CMS, however these were developed considering only shallow, crustal events [1]. Whether or not these correlations and corresponding equations are valid for other tectonic regimes, such as subduction zones, is currently unknown. One study has investigated the correlation of response spectral values in Japanese ground motions and compared them to the Baker and Jayaram [3] correlation coefficients [5]. It was concluded that the spectral correlations in the Japanese motions were similar to those developed by Baker and Jayaram, and these spectral correlations could be used as a viable surrogate for Japanese motions. The database considered comprised of crustal and subduction zone (interface and interslab) events; however, the largest earthquake in the database was the 2003 M_w = 8.0 Tokachi-Oki earthquake [5].

This paper evaluates the response correlation values from a large database of worldwide subduction zone earthquakes, including the 2011 M_w = 9.0 Tohoku earthquake. The results are then compared to the correlations observed by Baker and Jayaram [3] for shallow, crustal events. The results can be used to develop CS and CMS in worldwide subduction tectonic zones, such as those found in South and Central America, Japan, and the Pacific Northwest of North America.

2. Subduction Zone Ground Motion Database

The ground motion database used for this study comprises 2200 tri-directional records recorded in worldwide subduction regimes. As shown in Table 1, many of the records were from Japan; however, there were also historic records from South, Central, and North America. The Japanese records were obtained from the K-Net database [6]; the other records were obtained primarily from the United States Geological Survey (USGS) through the COSMOS Virtual Data Center [7]. Only free-field, surface records were considered. Most of the USGS records were downloaded as filtered and corrected, and thus, required no further modification. The K-Net records were baseline corrected and filtered with a 4th order Buttersworth bandpass filter with cutoff frequencies of 0.1 and 25 Hz.

The fault plane determined by the Geospatial Information Authority of Japan (GIS) was used to calculate the closest distance to fault (R_{cd}) for the K-Net records when available. For other records, the hypocentral distance was combined with an estimate of the rupture dimensions calculated with magnitude-area relations for subduction zone events in order to estimate an R_{cd} distance [8].

Many of the GMPEs considered also require a site classification or 30m average shear wave velocity (*Vs30*). For the K-Net stations, where only the 20m average shear wave velocity (*Vs20*) was recorded, *Vs30* values were inferred using the model developed by Kanno et al. [9]. For other stations with limited shear wave velocity measurements, the model proposed by Boore [10] was utilized to predict *Vs30*.

Table 1 – Record database summary

Event	Magnitude (M_w)	Year	Number of Records
Geiyo, Japan	6.8	2001	316
Guerrero, Mexico	6.6	1994	13
Michoacan, Mexico	7.1	1997	14
El Salvador	7.6	2001	44
Miyagi-Oki, Japan	7.2	2005	456
Puget Sound, Washington	6.7	1965	2
Olympia, Washington	7.1	1949	2
Nisqually, Washington	6.8	2001	37
Hokkaido, Japan	8.0	2003	358
Tohoku, Japan	9.0	2011	701
El Maule, Chile	8.8	2010	28
Michoacan, Mexico	8.1	1985	13
Iquique, Chile	8.2	2014	2
Southern Sumatra, Indonesia	8.4	2007	1

3. Spectral Correlation Calculations

A GMPE typically has the following form:

$$\ln Sa(T) = \mu_{\ln Sa}(M,R,\theta,T) + \sigma_{\ln Sa}(M,R,\theta,T) \times \varepsilon(T) \quad (1)$$

Where $\mu_{\ln Sa}(M,R,\theta,T)$ and $\sigma_{\ln Sa}(M,R,\theta,T)$ are the mean and standard deviation of the natural log of spectral acceleration (Sa) predicted by the GMPE at a certain period: T. These depend on the magnitude of the event: M, some distance metric: R, the period of interest: T, and any number of other parameters: θ. These parameters may include local site conditions (i.e. site class or *Vs30*), event type (i.e. interface or intraslab), location, etc. The term $\varepsilon(T)$ defines the number of standard deviations by which lnSa deviates from the predicted mean: $\mu_{\ln Sa}$. For an observed ground motion with known Sa(T), M, R and θ, $\varepsilon(T)$ is determined simply by calculating the number of standard deviations that the observed Sa(T) varies from the mean predicted $\mu_{\ln Sa}$ from a specific GMPE. This is shown mathematically by rearranging Eq. (1) as:

$$\varepsilon(T) = [\ln Sa(T) - \mu_{\ln Sa}(M,R,\theta,T)]/\sigma_{\ln Sa}(M,R,\theta,T) \quad (2)$$

In this study, the $\varepsilon(T)$ for a variety of periods is calculated for each ground motion in the database, using a variety of GMPEs to determine $\mu_{\ln Sa}$ and $\sigma_{\ln Sa}$. Then, the spectral correlations between different periods are calculated using the Pearson product-moment correlation coefficient [11].

4. Correlation Results

The following section presents the epsilon correlation coefficients calculated from the ground motion database described previously.

Fig. 1a presents the epsilon correlation coefficients calculated for the entire database of. Each line in Fig. 1 represents a different value of T_2. The x-axis represents values of T_1, while the y-axis represents the epsilon correlation coefficient, $\rho_{\varepsilon(T1),\varepsilon(T2)}$, between T_2 and T_1. The GMPE developed by Zhao et al. [12] was used to predict geometric mean (geomean) spectral accelerations and standard deviations for the ground motions at different periods for use in Eq. (2). Zhao et al. [12] provide an empirical GMPE for both interface and intraslab subduction events based on Japanese earthquake data. It was considered here initially because it can be used for both interface and intraslab events, and because the considered database is dominated by Japanese events. Fig. 1b illustrates the epsilon correlation coefficients predicted using the Baker and Jayaram [3] model, which is based on crustal events primarily from North America. Similar trends can be observed when comparing Figs 1a and 1b, although differences can be observed when T_1 is small (<0.5sec) and T_2 is large.

The format of Fig. 1 and subsequent figures is based on that from a study by Jayaram et al. [5].

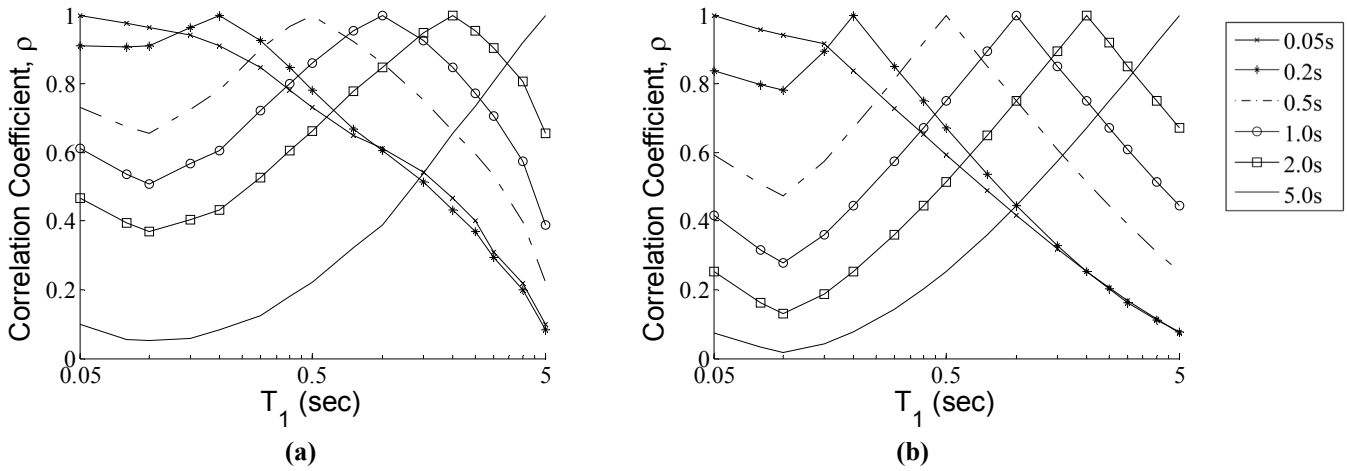

Fig. 1 - Epsilon correlation coefficient, $\rho_{\varepsilon(T1),\varepsilon(T2)}$, plots between T_2 and T_1 calculated using the Zhao et al. [12] GMPE for (a) the entire subduction zone record database and (b) predicted by the Baker and Jayaram [3] shallow crustal correlation model.

Similarly, Figs. 2a and 2b present the epsilon correlation coefficient plots for the interface and intraslab events, respectively. These results are similar to those observed in Fig. 1. The major difference between the two record subsets appears to be stronger correlations between T_2 and T_1 for the subduction records when the two periods are far apart.

To further compare the epsilon correlation coefficients observed between the record subsets and the Baker and Jayaram [3] correlation model, an "acceptance region" was constructed around each line in Fig. 2. These acceptance regions express the uncertainty in the correlation estimates due to the limited number of ground motion records. The uncertainty is inversely proportional to the number of records, i.e., fewer records produces less certain results. The acceptance regions are developed around one set of observations (i.e. epsilon correlation coefficients observed for the interface records) so that if the second set of observations (i.e. epsilon correlation coefficients predicted using the Baker and Jayaram [3] model) falls outside the region, then there is less than a 5% chance that the difference is due solely to the limited number of records. In other words, the acceptance region provides a 95% confidence interval around the first set of observations.

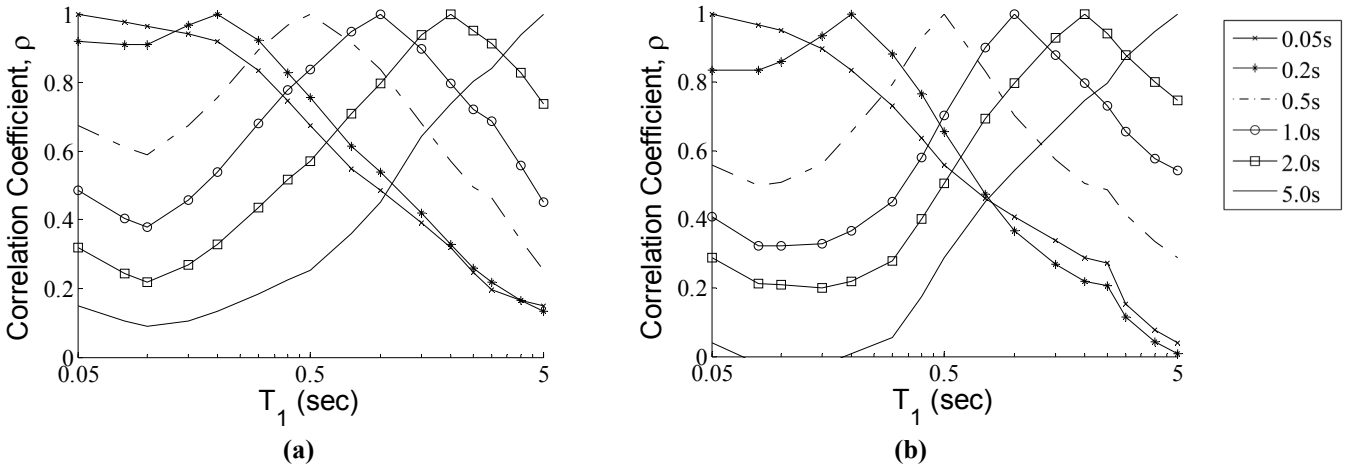

Fig. 2 - Epsilon correlation coefficient, $\rho_{\varepsilon(T1),\varepsilon(T2)}$, plots between T_2 and T_1 calculated using the Zhao et al. [12] GMPE for (a) the interface records and (b) the intraslab records.

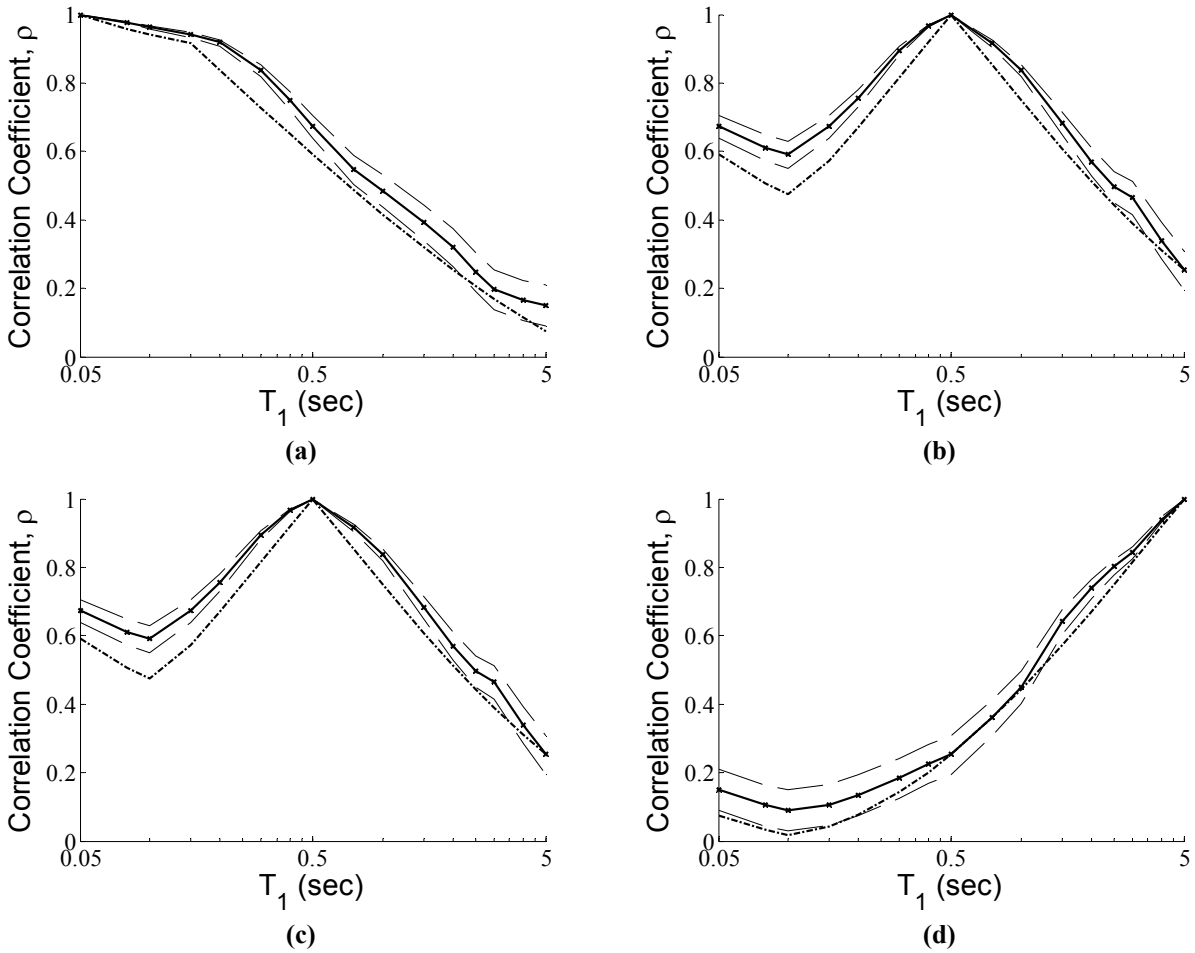

Fig. 3 - Epsilon correlation coefficient, $\rho_{\varepsilon(T1),\varepsilon(T2)}$, plots between T_2 and T_1 calculated using the Zhao et al. [12] GMPE for the interface database compared to the Baker and Jayaram [3] predictions for (a) T_2 = 0.05 seconds, (b) T_2 = 0.5 seconds, (c) T_2 = 2.0 seconds, and (d) T_2 = 5.0 seconds. ━●━ Correlation calculated using the Zhao et al. [12] GMPE; ╌▬╌▬ Correlation calculated using the Baker and Jayaram [3] predictions; ▬ ▬ Boundary of acceptance regions.

Fig. 3 presents the subduction database results, including the acceptance region, for T_2 = 0.05, 0.5, 2.0, and 5.0 seconds compared to the Baker and Jayaram [3] predictions. Similarly, Fig. 4 presents similar results for the intraslab database. Fig. 4 shows a high degree of conformity between the observed epsilon correlation coefficients for the intraslab database and the Baker and Jayaram [3] predictions, meaning that the Baker and Jayaram [3] model is a suitable surrogate for predicting epsilon correlations for worldwide intraslab events. Fig. 3 shows a less good match when considering the interface database – however, the results indicate that the Baker and Jayaram [3] model, while less accurate, still provides reasonably close results to those observed while using the interface record database.

4.1 Other Subduction Zone GMPEs

Also of interest is the effect on the epsilon correlation coefficients when considering other GMPEs. There are a large number of subduction zone GMPEs that have been developed by researchers using different suites of motions and different parameters. In this study, five modern subduction zone GMPEs are considered as summarized in Table 2.

The results observed using the Zhao et al. [12] GMPE were presented in Fig. 1 and Fig. 2. Fig. 5 illustrates the results observed from the remaining four GMPEs.

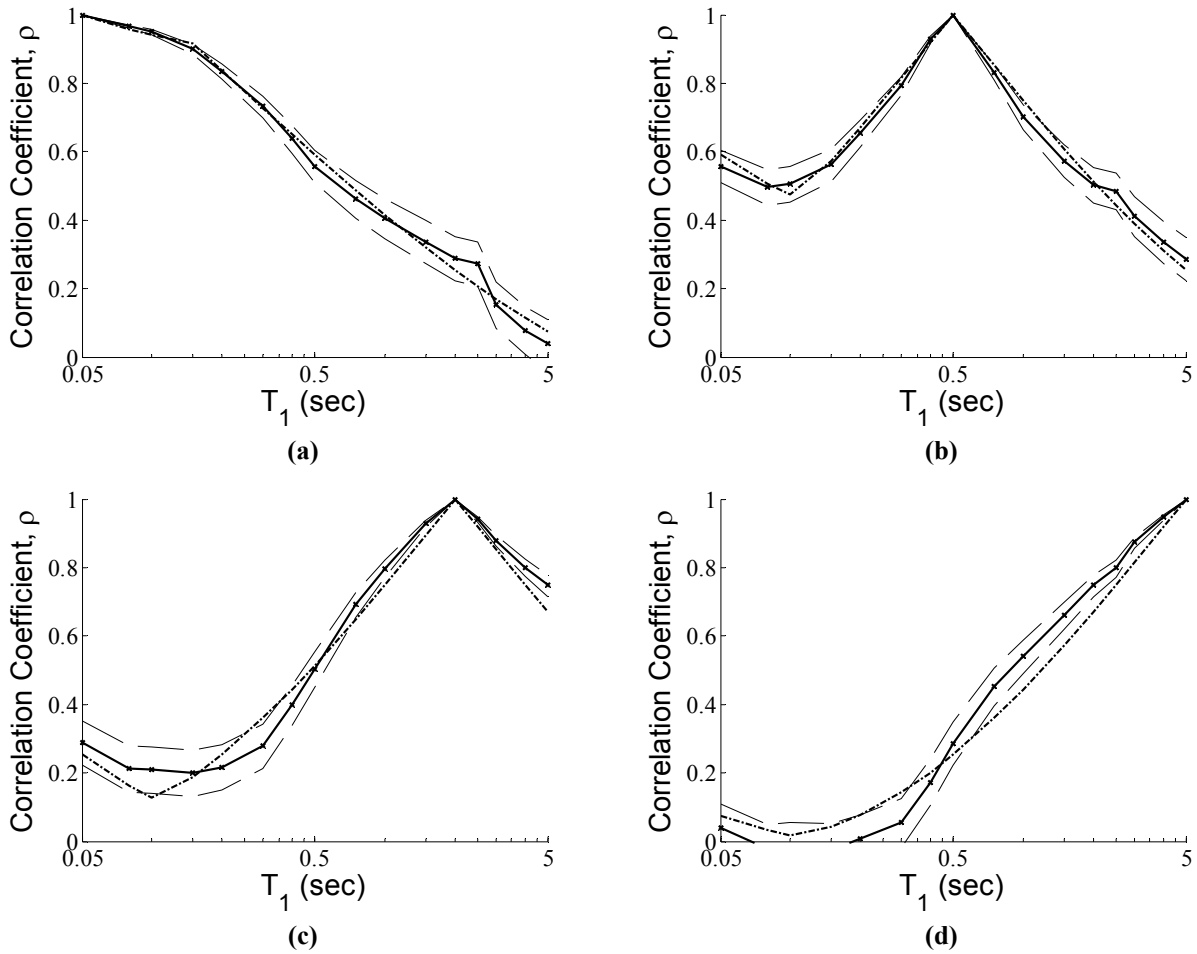

Fig. 4 - Epsilon correlation coefficient, $\rho_{\varepsilon(T1),\varepsilon(T2)}$, plots between T_2 and T_1 calculated using residuals of the Zhao et al. [12] GMPE for the intraslab database compared to the Baker and Jayaram [3] predictions for (a) T_2 = 0.05 seconds, (b) T_2 = 0.5 seconds, (c) T_2 = 2.0 seconds, and (d) T_2 = 5.0 seconds. —*— Correlation calculated using the Zhao et al. [12] GMPE; - - - Correlation calculated using the Baker and Jayaram [3] predictions; — — Boundary of acceptance regions.

Table 2 – Summary of Modern Subduction Zone GMPEs Considered

Authors(s)	Year	Source Type
Zhao et al.	2003	Interface/Intraslab
Atkinson and Macias	2009	Interface
Ghofrani and Atkinson	2014	Interface
Addo et al. (BC Hydro Model)	2012	Interface/Intraslab
Atkinson and Boore global model	2003	Interface/Intraslab

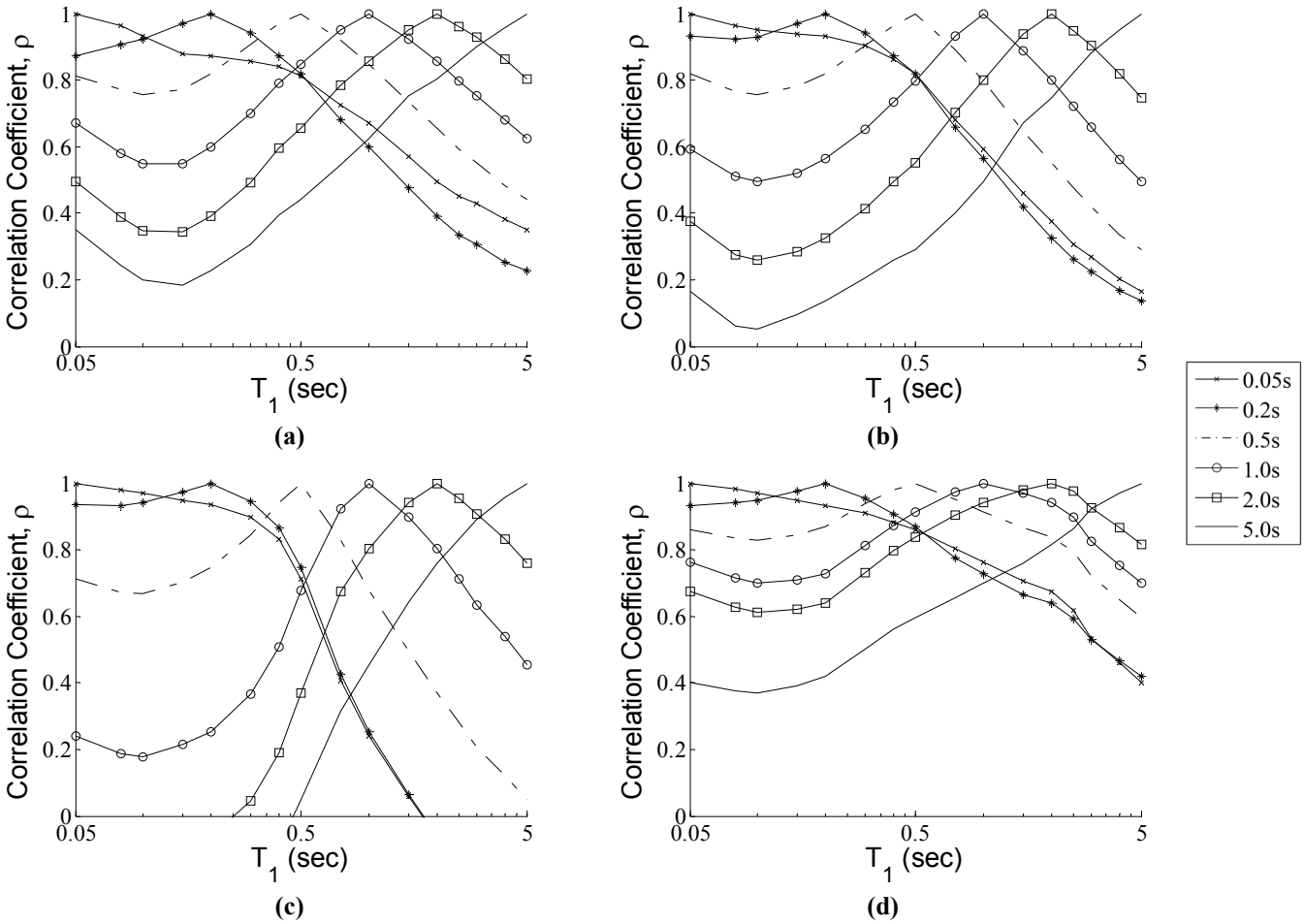

Figure 5 - Epsilon correlation coefficient, $\rho_{\varepsilon(T1),\varepsilon(T2)}$, plots between T_2 and T_1 calculated using the (a) Atkinson and Macias [13], (b) Ghofrani and Atkinson [14], (c) Addo et al. [15], and (d) Atkinson and Boore global GMPE [16].

4.2 Combined GMPEs

Typically, in probabilistic seismic hazard analysis (PSHA) models multiple applicable GMPEs will be weighted and combined for ground motion prediction. This is done in order to better account for the epistemic uncertainty involved in the estimation of ground motion attenuation from source to site.

Both the Geological Survey of Canada (GSC) and the United States Geological Survey (USGS) have used this method in their latest PSHA models. Tables 3 and 4 summarize the considered GMPEs and their respective weights for the GSC 2015 [17] and USGS 2014 [18] intraslab and interface GMPEs, respectively. These GMPE were used in the development of the latest national seismic hazard maps in Canada and the United States.

Table 3 – Summary of GSC (2015) and USGS (2014) Intraslab GMPE Weights

GMPE	GSC 2015 Weight	USGS 2014 Weight
Zhao et al. (2003)	1	0.33
Addo et al. (BC Hydro Model; 2012)	0	0.33
Atkinson and Boore global model (2003)	0	0.167
Atkinson and Boore Cascadia model (2003)	0	0.167

Table 4 – Summary of GSC (2015) and USGS (2014) Interface GMPE Weights

GMPE	GSC 2015 Weight	USGS 2014 Weight
Zhao et al. (2003)	0.1	0.3
Addo et al. (BC Hydro Model; 2012)	0.2	0.3
Atkinson and Macias (2009)	0.5	0.3
Ghofrani and Atkinson (2014)	0.2	0
Atkinson and Boore global model (2003)	0	0.1

The epsilon correlation coefficients computed using these two combined GMPEs are summarized in Fig. 6 and Fig. 7 for intraslab and interface events, respectively.

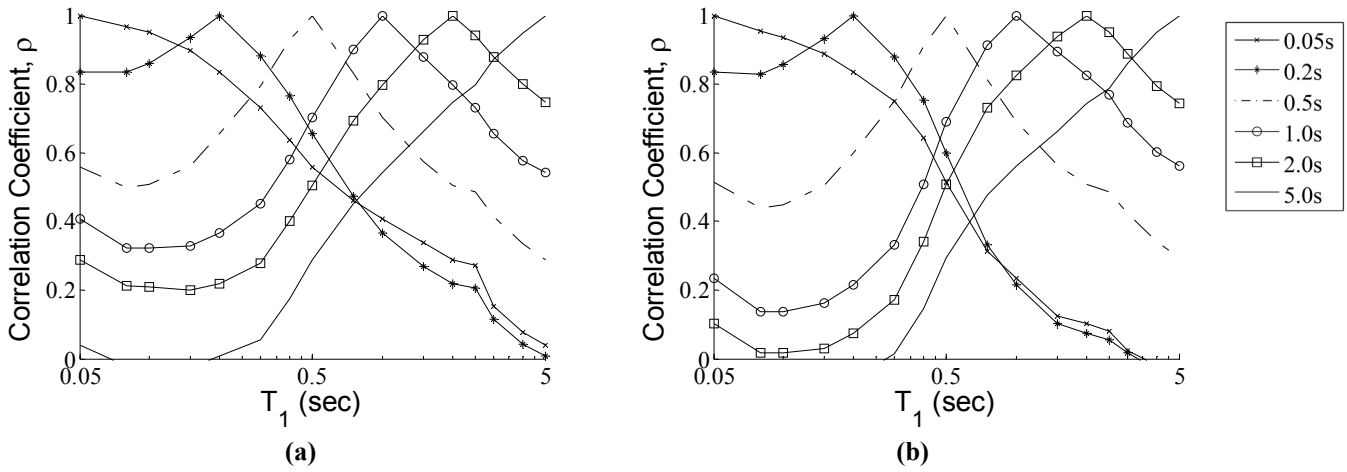

Fig. 6 - Epsilon correlation coefficient, $\rho_{\varepsilon(T1),\varepsilon(T2)}$, plots between T_2 and T_1 calculated using residuals of the (a) GSC 2015 Intraslab GMPE and (b) USGS 2014 Intraslab GMPE.

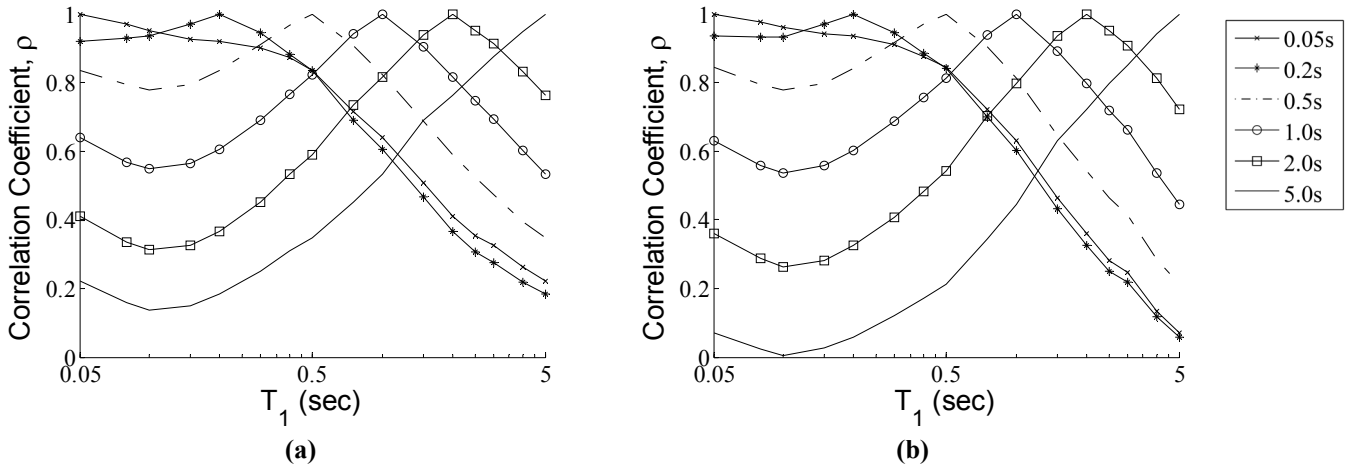

Fig. 7 – Epsilon correlation coefficient, $\rho_{\varepsilon(T1),\varepsilon(T2)}$, plots between T_2 and T_1 calculated using the (a) GSC 2015 Interface GMPE and (b) USGS 2014 Interface GMPE.

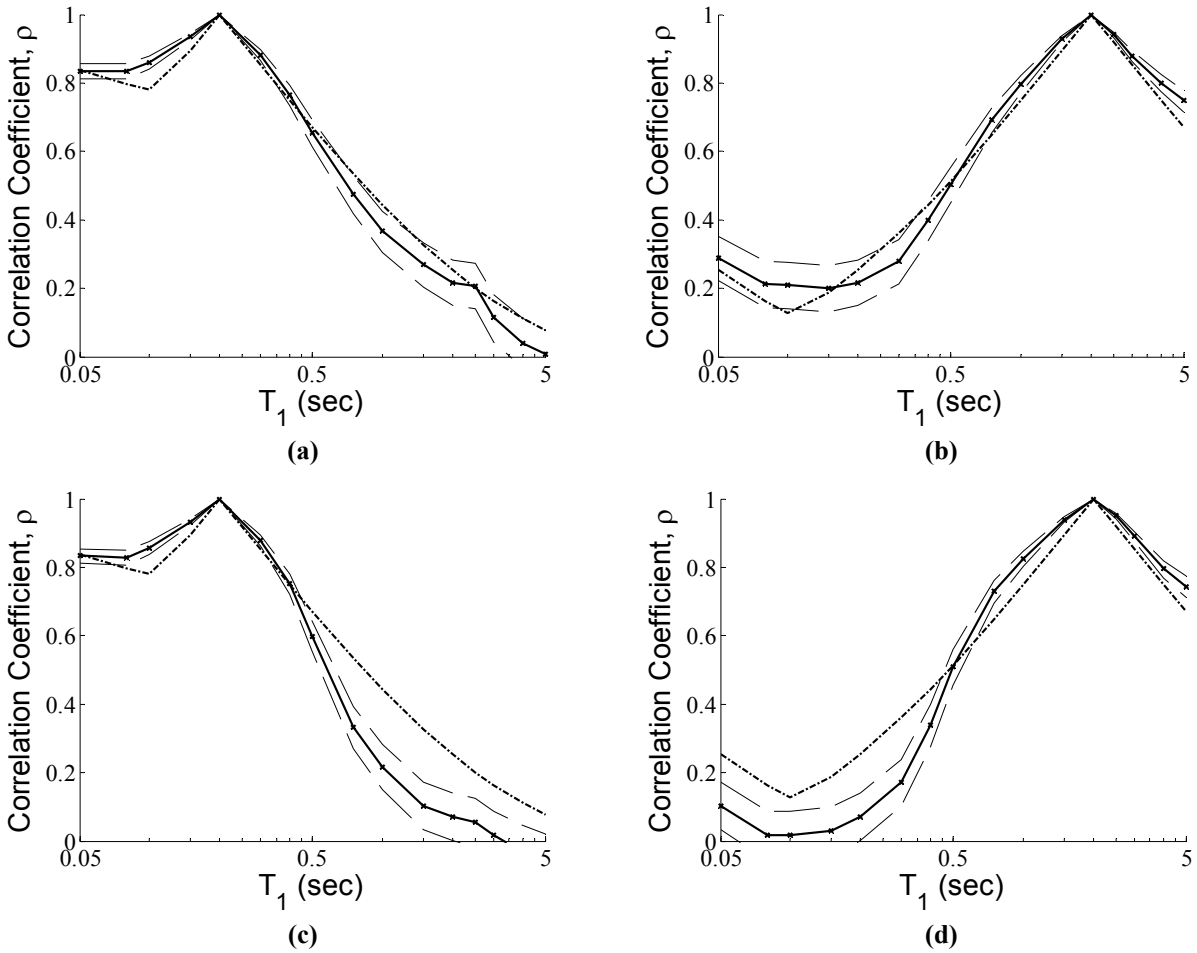

Fig. 8 - Epsilon correlation coefficient, $\rho_{\varepsilon(T1),\varepsilon(T2)}$, plots between T_2 and T_1 calculated using the Baker and Jayaram [3] predictions for compared to (a) GSC 2015 GMPE for the intraslab database at T_2 = 0.2 seconds, and (b) T_2 = 2.0 seconds; (c) USGS 2014 GMPE for the intraslab database at T_2 = 0.2 seconds, and (d) T_2 = 2.0 seconds. —x— Correlation calculated using the combined GMPE; - - - Correlation calculated using the Baker and Jayaram [3] predictions; — —Boundary of acceptance regions

Fig. 6 and Fig. 7 show similar trends between the two combined GMPEs. Comparing the results in Fig 6. for intraslab events to the Baker and Jayaram [3] correlation coefficients (Fig. 1b) reveals a relatively good match when using the GSC 2015 intraslab GMPE. However, when using the USGS 2014 intraslab GMPE, the observed epsilon correlations are lower, on average, than the Baker and Jayaram [3] coefficients. This is illustrated in Fig. 8 for T_2 = 0.2 and 2.0 seconds.

A similar comparison is made for the two combined interface GMPEs in Fig. 9. From this figure it can be seen that the Baker and Jayaram [3] correlation coefficients are, on average, lower than the observed interface correlations and outside of the acceptance region.

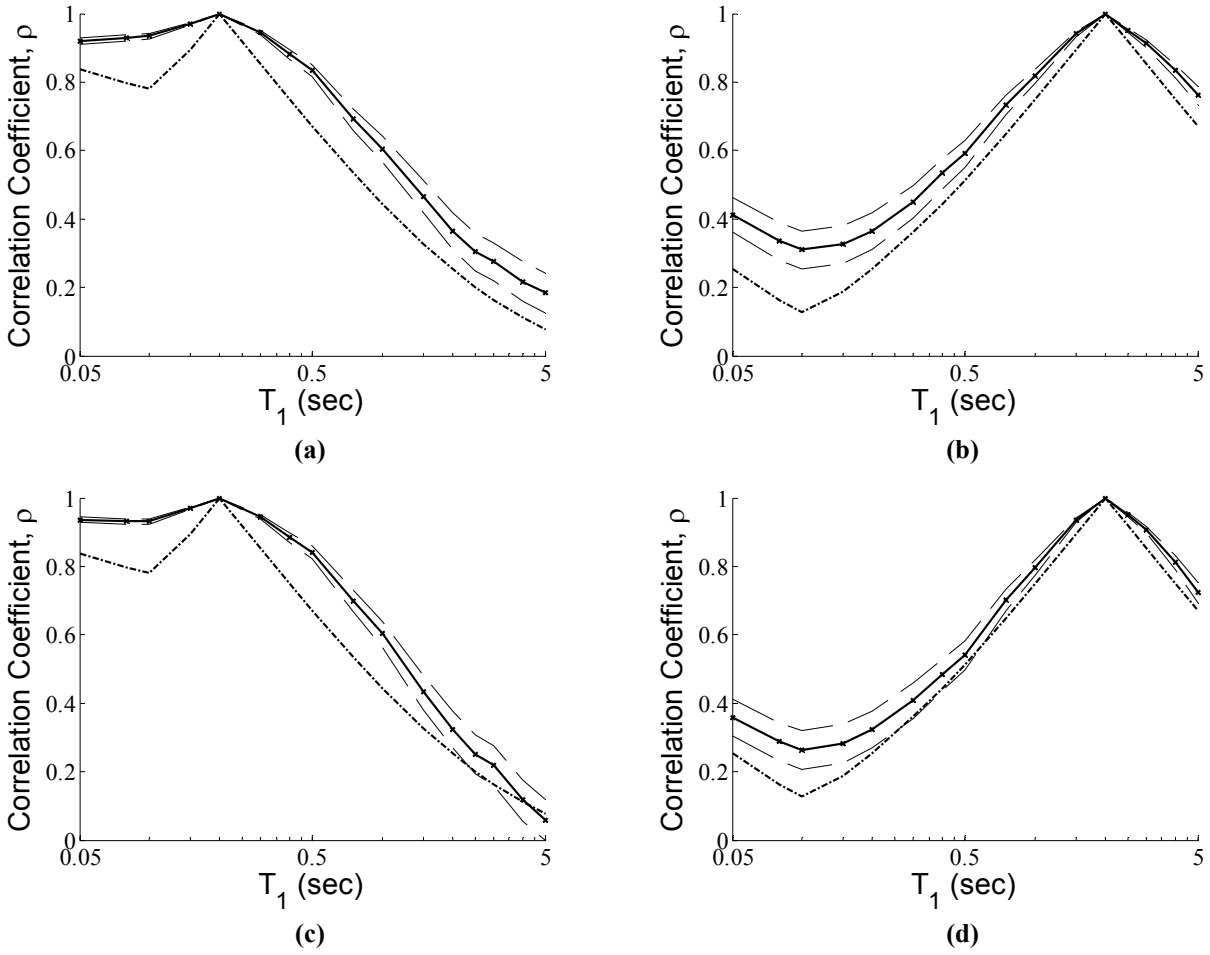

Fig. 9 - Epsilon correlation coefficient, $\rho_{\varepsilon(T1),\varepsilon(T2)}$, plot between T_2 and T_1 calculated using the Baker and Jayaram [3] predictions for compared to (a) GSC 2015 GMPE for the interface database at T_2 = 0.2 seconds, and (b) T_2 = 2.0 seconds; (c) USGS 2014 GMPE for the interface database at T_2 = 0.2 seconds, and (d) T_2 = 2.0 seconds. —*— Correlation calculated using the combined GMPE; - - - Correlation calculated using the Baker and Jayaram [3] predictions; —— Boundary of acceptance regions

5. Conclusions

In this study a database of worldwide subduction zone (both interface and intraslab) events was studied to determine their epsilon correlation coefficients. The database comprised several large magnitude events including the 2010 M_w = 9.0 Tohoku, Japan earthquake.

The observed correlations were compared to the Baker and Jayaram [3] epsilon correlations, which are commonly used to develop CS and CMS. Using the Zhao at al. [12] GMPE to calculate epsilon values, it was observed that the Baker and Jayaram correlation coefficients matched well with the observed values. This means

that the Baker and Jayaram coefficient equations would be a suitable surrogate for these types of events. Several other modern subduction GMPEs were also used to calculate epsilon values. Some produced similar results to those observed using Zhao et al. GMPE, while others predicted much higher or lower correlations.

Next, the GSC 2015 and USGS 2014 subduction GMPEs, which comprise a weighted average of several GMPEs, were used to calculate epsilon values for the record database. For each record type (interface or intraslab) the two GMPEs produced similar results, which were comparable to the Baker and Jayaram [3] correlation values (although not strictly within the 95% confidence acceptance region). Due to these findings, it may be acceptable to use the Baker and Jayaram [3] epsilon correlation coefficients when developing CS or CMS for subduction zone events in the Northwest Pacific United States and Southwesten Canada. However, for more accurate results, interface or intraslab specific correlation coefficients could be used.

6. Acknowledgements

The authors would like to thank Dr. Jason Dowling for the implementation of various GMPEs and Prof. Liam Finn for his support and encouragement through this study.

7. References

[1] Bozorgnia Y, Abrahamson NA, Atik LA, Ancheta TD, Atkinson GM, Baker JW, ... Youngs R (2014). NGA-West2 research project. *Earthquake Spectra*, **30** (3), 973-987.

[2] Baker JW, Cornell CA (2006a). Correlation of response spectral values for multicomponent ground motions. *Bulletin of the Seismological Society of America*, **96** (1), 215-227.

[3] Baker JW, Jayaram N (2008). Correlation of spectral acceleration values from NGA ground motion models. *Earthquake Spectra*, **24** (1), 299-317.

[4] Baker JW, Cornell CA (2006b). Spectral shape, epsilon and record selection. *Earthquake Engineering & Structural Dynamics*, **35** (9), 1077-1095.

[5] Jayaram N, Baker JW, Okano H, Ishida H, McCann Jr MW, Mihara Y (2011). Correlation of response spectral values in Japanese ground motions. *Earthquakes and Structures*, **2** (4), 357-376.

[6] Kinoshita S (1998). Kyoshin net (K-net). *Seismological Research Letters*, **69** (4), 309-332.

[7] Archuleta RJ, Steidl J, Squibb M (2006). The COSMOS virtual data center: a web portal for strong motion data dissemination. *Seismological Research Letters*, **77** (6), 651-658.

[8] Strasser FO, Arango MC, Bommer JJ (2010). Scaling of the source dimensions of interface and intraslab subduction-zone earthquakes with moment magnitude. *Seismological Research Letters*, **81** (6), 941-950.

[9] Kanno T, Narita A, Morikawa N, Fujiwara H, Fukushima Y (2006). A new attenuation relation for strong ground motion in Japan based on recorded data. *Bulletin of the Seismological Society of America*, **96** (3), 879-897.

[10] Boore DM (2004). Estimating Vs30 (or NEHRP site classes) from shallow velocity models (depths < 30 m). *Bulletin of the Seismological Society of America*, **94** (2), 591-597.

[11] Kutner MH, Nachtsheim C, Neter J (2004). *Applied linear regression models*. McGraw-Hill/Irwin.

[12] Zhao JX, Zhang J, Asano A, Ohno Y, Oouchi T, Takahashi T, ... Fukushima Y. (2006). Attenuation relations of strong ground motion in Japan using site classification based on predominant period. *Bulletin of the Seismological Society of America*, **96** (3), 898-913.

[13] Atkinson GM, Macias M (2009). Predicted ground motions for great interface earthquakes in the Cascadia subduction zone. *Bulletin of the Seismological Society of America*, **99** (3), 1552-1578.

[14] Ghofrani, H, Atkinson GM (2014). Ground-motion prediction equations for interface earthquakes of M7 to M9 based on empirical data from *Japan.Bulletin of Earthquake Engineering*, **12** (2), 549-571.

[15] Addo KO, Abrahamson NA, Youngs RR (2012). Probabalistic Seismic Hazard Analysis (PSHA) Model – Volume 3: Ground Motion Characterization (GMC) Model. *BC Hydro Engineering Report E658*.

[16] Atkinson GM, Boore DM (2003). Empirical ground-motion relations for subduction-zone earthquakes and their application to Cascadia and other regions. *Bulletin of the Seismological Society of America*, **93** (4), 1703-1729.

[17] Halchuk S, Allen TI, Adams J, Rogers GC (2014). Fifth Generation Seismic Hazard Model Input Files as Proposed to Produce Values for the 2015 National Building Code of Canada. *Geological Survey of Canada Open File 7576*.

[18] Petersen MD, Moschetti MP, Powers PM, Mueller CS, Haller KM, Frankel AD, … Olsen AH (2014) Documentation for the 2014 update of the United States national seismic hazard maps. *U.S. Geological Survey Open-File Report 2014–1091*, 243 p. *http://dx.doi.org/10.3133/ofr20141091*.